

QUANTUM MEMORY WITH HOT CESIUM ATOMS

MATEVŽ VAUPOTIČ

Fakulteta za matematiko in fiziko
Univerza v Ljubljani

Quantum memory (QM) is a subject of growing scientific and technological interest due to the accelerated development of quantum networks and quantum computing. Electromagnetically induced transparency (EIT) conducted on hot atoms offers a relatively simple technological realisation of quantum memory and is therefore very promising for future scalability and mass production. This article focuses on the theoretical background of EIT-based QM and its application in research conducted at the Laboratory for cold atoms at the Jožef Stefan Institute. In the experiment, EIT in a cesium vapor at room temperature is studied, where the ground, excited, and storage states of cesium atoms form a three-level Λ -system. Successful storage of light for a few μs was demonstrated using this method.

KVANTNI SPOMIN Z VROČIMI CEZIJEVIMI ATOMI

Kvantni spomin (QM) je predmet vse večjega znanstvenega in tehnološkega zanimanja zaradi pospešenega razvoja kvantnih omrežij in kvantnega računalništva. Elektromagnetno inducirana prosojnost (EIT), izvedena na vročih atomih, omogoča tehnološko razmeroma preprosto izvedbo kvantnega spomina, kar predstavlja dobre obete za množično proizvodnjo in uporabo. Članek se osredotoča na teoretično ozadje kvantnega spomina na osnovi EIT in na uporabo tega v raziskavah, ki potekajo v Laboratoriju za hladne atome na Institutu Jožefa Stefana. Eksperiment obravnava EIT na cezijevi pari pri sobni temperaturi, kjer osnovno, vzbujeno in spominsko stanje cezijevih atomov tvorijo trinivojski sistem Λ . Raziskava uspešno demonstrira shranjevanje svetlobe za nekaj μs s to metodo.

1. Introduction: Why do we need quantum memory?

In quantum computing, a **qubit** (abbreviation for quantum bit) is a basic unit of quantum information. A qubit is a two-state quantum-mechanical system. Two good examples are the spin of the electron, where the two levels can be understood as spin up and spin down; or the polarization of a single photon in which the two spin states (left-handed and right-handed circular polarization) can also be measured as horizontal and vertical linear polarization [1, 2].

Quantum communication is the exchange of qubits between multiple participants. One practical application of this is quantum cryptography. The best-known security protocol in quantum cryptography is quantum key distribution (QKD). It enables two parties to generate a shared random secret key known only to them. This key can then be used with any encryption algorithm to encrypt (and decrypt) a message, which can then be transmitted over a standard communication channel. If a hypothetical third party attempts to intercept the quantum information, it will perform a quantum measurement, causing the wave function carrying the information to collapse. The communicating parties would recognize this as a significant enough difference between the information sent and received and adjust the exchange of the encryption key accordingly, ultimately keeping the communication secure [3, 4]. Consequently, quantum communication is exceptionally secure compared to classical methods and significant investments are being made worldwide in its development. Several implementations have already been realized since the early 2000s [4].

However, quantum communication is not exempt from (ubiquitous) attenuation, so that losses due to photon absorption in optical fibers and quantum decoherence only allow reliable transmission over limited distances [5]. For arbitrarily long distances, intermediate stations, so-called trusted nodes, are necessary to divide these distances into sufficiently short sections for QKD to still function well. At these points, the quantum information is temporarily converted into classical information due to current technological limitations, which represents a weak point in the communication line. This problem could be solved with quantum repeaters. Unlike trusted nodes, these devices store

qubits so that the quantum nature of the information is preserved at all times. An essential component of a quantum repeater is, therefore, a **quantum memory**, a device that can temporarily store quantum states and retrieve them at a later time, which finally leads us to our topic.

2. Quantum memory

2.1 Definition

Quantum memory is a device that enables the storage of quantum information and its later retrieval (see Figure 1). An informational qubit is prepared using a particle with two distinct quantum states. The biggest challenge in building such a device is the collapse of the wave function after a measurement is made, hence, no measurements can be performed on the qubit itself. Instead, the information of the qubit must be transferred directly to the matter using specific physical phenomena [6, 7]. With this in mind, let us now take a detailed look at what quantum memories should be, could be, and what they currently are.

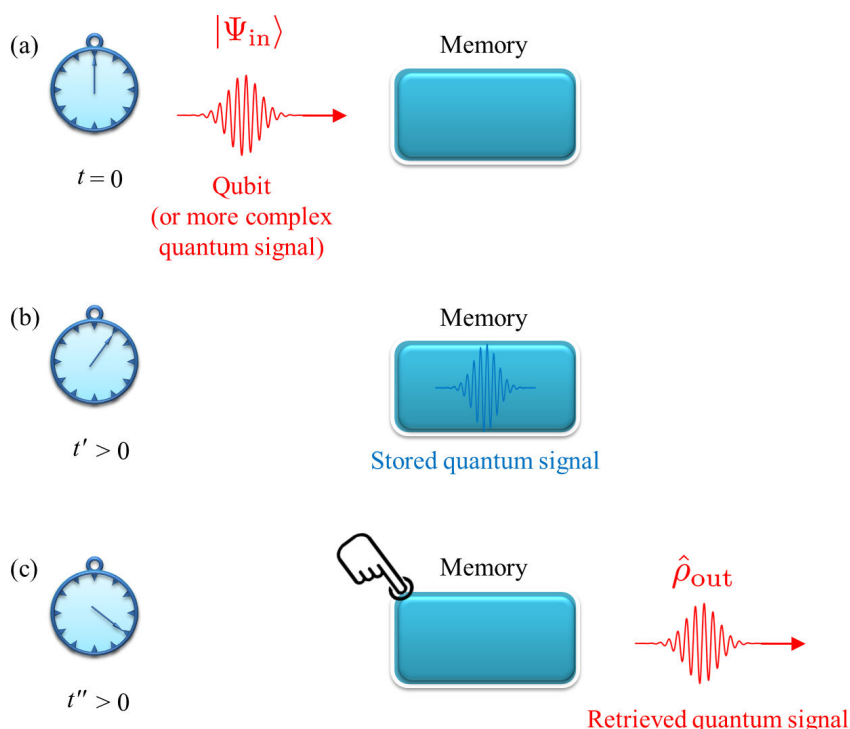


Figure 1. General concept of a quantum memory. (a) At time $t = 0$, a qubit arrives at the memory to which it is transferred. (b) The qubit remains stored in the memory for an arbitrary time. (c) At a later time t'' , when the user “pushes a button”, the quantum state is released from the memory. If the storage time t'' exceeds the memory lifetime τ , then the parameters of QM start to deteriorate. Adapted from [6].

2.2 Requirements

There are many different approaches to implementing quantum memory, so there is a need for a system of standard parameters that we can use to compare these different approaches. The following parameters are the main assessment criteria for a quantum memory:

- **Fidelity** (F) quantifies how closely the retrieved quantum state matches the input state. It can be a good measure of *how quantum-like* a memory really is [8].
- **Efficiency** (η) represents the energy ratio between the retrieved and input states. To minimize additional transmission losses, the efficiency should be close to 100%.

- **Memory time** (τ) – or storage time – refers to the duration over which a quantum state remains reliably stored, with decoherence limiting the storage time and affecting both fidelity and efficiency. In practical quantum communication schemes, memory times of a few tens of milliseconds to a few seconds are required, depending on the protocol and length of the communication link.
- **Multimode capacity** denotes the number of elementary quantum states that a memory can store in parallel, which increases the speed and efficiency of quantum communication protocols.
- **Wavelength** of fiber-optics quantum communication. Memories should ideally operate at telecommunication wavelengths ($\lambda = 1.3$ to $1.5 \mu\text{m}$), although quantum interfaces can convert photons between telecommunication and visible wavelengths.
- **Bandwidth** of quantum memory. This describes the spectral width of the photons that a quantum memory can store. In general, larger bandwidths are desirable, but in practice they are always limited depending on the different QM approaches.
- **Signal-to-noise ratio** – Quantum memories often use bright auxiliary beams in addition to single-photon signals, which require strict noise suppression to preserve the quantum nature of the signal. Excess noise can obscure the “*quantumness*” of the stored information [6].

Individual QM systems are usually optimized for some of these parameters, but currently, none can optimize all parameters simultaneously. In the following, we will mainly focus on the **storage time** parameter, as this parameter is currently the limiting factor of most QM implementations.

2.3 Quantum memory protocols

Before focusing on one of the most promising mechanisms – electromagnetically induced transparency (EIT) – let us first list different types of QM approaches that are currently under investigation.

The first and simplest idea for QM would – of course – be a sufficiently long fiber loop in which an incoming photon is diverted into the delay loop by means of a switch and later released. However, this approach does not yield sufficient efficiency, which is mainly due to the reflection and transmission losses of the various optical components [9].

Quantum memories can be broadly categorized into two main types: single quantum emitter-based and ensemble-based approaches. These categories differ in the physical substrates used to store quantum information and the protocols that enable the mapping of quantum states onto these substrates [6].

Single quantum emitter-based memories store information in isolated quantum systems. These systems are ideal for fundamental quantum experiments and specific applications such as high-fidelity qubit storage and long-distance entanglement. Existing protocols are:

- **Single atoms in cavities:** Optically trapped single atoms in cavities have been used to demonstrate polarization qubits storage [10] and matter-matter entanglement generation.
- **Individual trapped ions:** Individually addressable ions exhibit long coherence times and enable teleportation of qubits and state mapping from photons to ions with 95% fidelity but low efficiency [11].
- **Nitrogen-vacancy centers in diamonds:** Nitrogen-vacancy centers (NVCs) are naturally occurring or engineered defects in bulk diamonds that exhibit rich quantum properties. They enable photon-spin entanglement, the transfer of states to nuclear spins with coherence times in the

millisecond range, and long-distance entanglement between NVCs. The disadvantages of these applications are the long radiation lifetime of NVCs and the strong phonon sideband in their emission spectrum [12].

- **Quantum dots:** These are semiconductor particles (a few nanometers in size) with optical and electronic properties that differ from those of larger particles due to quantum mechanical effects. They are studied as potential QM systems [13].

Ensemble-based memories utilize the collective properties of many particles to store quantum states. These systems support multimode storage and offer a variety of very different protocols:

- **Cold or ultra-cold atomic gasses:** They were the earliest media used to store light. Very pure gasses of alkali atoms are prepared via laser cooling at various temperatures, from a few mK in magneto-optical traps to μK in dipole traps and even in the nK range in Bose-Einstein condensates (BEC). This protocol is also the focus of research interest at the Laboratory for cold atoms (JSI), where a storage time of more than 400 μs was achieved with a magneto-optical trap [14].
- **Hot atomic vapors:** Here “hot” refers to a temperature range above 300 K, which mostly means gasses at room temperature, enabling EIT- and Raman-based protocols and showing quantum behavior in optical storage experiments despite higher temperatures. This type of QM is much easier to implement as no laser cooling is required. It is the main topic of this article.
- **Rare-earth-doped crystals:** These materials can exhibit extremely long coherence times at cryogenic temperatures. They are therefore studied as versatile light storage media. EIT-based light storage in a crystal was demonstrated shortly after storage in atomic vapors.
- **Microcavity coupled NVC ensembles:** Theoretical proposals suggest that NV centers in diamond could also be used as a medium for ensemble-based memory [6].

2.4 Decoherence

Decoherence, the loss of quantum coherence, is the main obstacle to quantum memories and quantum information systems. It is the phenomenon that primarily limits storage times. While eigenstates of observables are relatively stable, superpositions of such states are vulnerable over time due to phase blurring. This process transforms pure quantum states into classical (non-quantum) mixed states and renders them useless for quantum purposes. Overcoming decoherence and controlling its sources is an important focus in quantum memory research. Despite the challenges involved, there are promising signs that systems can be found in which quantum states are preserved over an extended period of time [15].

When considering ensemble-based memories, inhomogeneities lead to different atoms (at different positions or with different velocities) evolving with uncorrelated individual phase factors. Since the re-emission process takes place as a collective in-phase emission of all atoms, uncontrolled dephasing stands in the way of this desired collective re-emission [7, 6]. From our own laboratory experience (see Chapter 4.), we can state that overcoming decoherence and controlling its sources is a crucial challenge in quantum memory research. In hot atoms QM, we try to reduce decoherence by adding the right amount of buffer gas to the cells, thus limiting the motion of atoms. In some cases, the choice of coating of the cell walls also plays a role, as it influences the interactions of the atoms with the cell walls during collisions. The most commonly used substances are paraffin or alkene coatings.

3. Electromagnetically induced transparency

One of the most promising mechanisms for the implementation of quantum memory is electromagnetically induced transparency (EIT). As the name suggests, it occurs in some media when a beam of light that should normally be absorbed is instead transmitted. Light propagating in an EIT medium experiences an extremely reduced group velocity. To store a light pulse with EIT, its group velocity is adiabatically reduced to zero as it propagates in the medium. This process transfers the quantum state of the light pulse into an atomic coherence [6]. EIT is the destructive quantum interference of two light fields in a three-level atomic energy structure. There are three possible configurations for a three-level structure, referred to as lambda (Λ), vee (V) and ladder, respectively, as shown in Figure 2. We will only focus on the lambda configuration as it is the most commonly used for the implementation of quantum memory and is also the one we use with ^{133}Cs in our experiment (see Chapter 4.1).

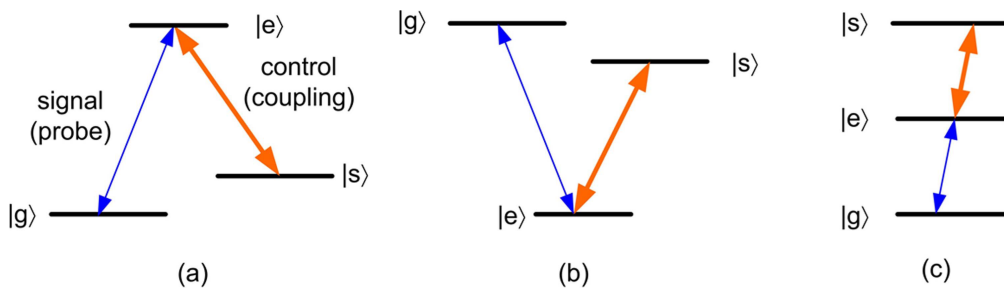


Figure 2. Three possible configuration of EIT, (a) lambda, (b) vee and (c) ladder. Adapted from [7].

Let us take a closer look at the energy level description of this phenomenon. We will name three levels that form a Λ -system: **ground** $|g\rangle$, **excited** $|e\rangle$, and **storage** $|s\rangle$. The atomic ensemble is illuminated with two lasers: a weak signal beam (also called *probe* beam) with a wavelength that corresponds to the transition between $|g\rangle$ and $|e\rangle$, and a strong control beam (also called *coupling* or *pump* beam) that corresponds to the transition between $|e\rangle$ and $|s\rangle$.

In the Λ -configuration, the transition between the two lower energy states, $|g\rangle$ and $|s\rangle$, is dipole-forbidden, so that the atoms can remain in these states for extended periods of time. Both states have allowed transitions to an excited state, $|e\rangle$. To modify the propagation of a signal beam that couples $|g\rangle$ and $|e\rangle$, a strong control beam is applied between $|s\rangle$ and $|e\rangle$. Each field resonates with the respective atomic transitions and is absorbed when applied individually. However, when both beams are present, they interfere destructively and prevent excitation to $|e\rangle$, so neither beam is absorbed [7]. Essentially, this is a two-photon process from $|g\rangle$ to $|s\rangle$ via $|e\rangle$.

If we want to retrieve the photon, we turn the control beam back on, and the atom transitions from the $|s\rangle$ state to the ground state via $|e\rangle$, emitting a photon with the same energy as the signal photon, which we proclaim as stored light. Although this explanation is intuitive and explains how the energy of the photon is conserved, it does not explain how the quantum information of the photons (i.e., polarization, etc.) is copied to an atomic ensemble [6, 16].

3.1 Slow light

Let us now try to understand how light is actually slowed down. Classically, to slow down light, we need to increase the refractive index of the medium through which the light passes, $n' = c_0/c$. However, the process is not straightforward, as we also need to consider what happens to the absorption in the medium when we do this. The complex refractive index is defined as $n = n' + in''$, where the real part n' describes the refraction and the imaginary part n'' describes the absorption.

The connection between the refractive index and the material's response to an electric field is established through the electric susceptibility $\chi(\omega)$, which is related to the electric permittivity as $\varepsilon(\omega) = 1 + \chi(\omega)$. Since the refractive index is related to the permittivity by $n = \sqrt{\varepsilon(\omega)}$, we can write $n \approx 1 + \frac{1}{2}\chi(\omega)$ by using a first-order expansion for small $\chi(\omega)$. If we take only the real part, we obtain the expression for the real refractive index

$$n' = 1 + \frac{1}{2}\text{Re}\chi(\omega). \quad (1)$$

This equation shows that the real part of the electric susceptibility determines how the light propagates in a medium. The imaginary part of $\chi(\omega)$, on the other hand, is responsible for absorption. Consequently, an increase in the refractive index alone does not necessarily lead to a sufficient slowing down of the light, as a higher n generally also leads to greater absorption.

However, there is a special regime in which this issue can be circumvented: We prepare the same configuration as in the previous section (a three-level Λ energy configuration illuminated by two beams). Absorption in the medium can occur when only one beam is active, but when both beams are active simultaneously, no atom can be in an excited state $|e\rangle$. As a result, no light can be absorbed and the medium becomes transparent. This phenomenon can be described quantitatively by the expression for linear susceptibility when the control beam is strong and its intensity is constant. By combining the Kramers-Kronig relations with the theory of Rabi oscillations and dressed states, the derivation [6, 7] yields

$$\chi(\omega) = g^2 N \frac{\gamma_{gs} + i\omega}{(\gamma_{ge} + i\omega)(\gamma_{gs} + i\omega) + |\Omega|^2}, \quad (2)$$

where γ_{gs} and γ_{ge} are the decoherence rates for the transitions $|g\rangle \rightarrow |s\rangle$ and $|g\rangle \rightarrow |e\rangle$, respectively, where in our case $\gamma_{gs} \rightarrow 0$, since the transition between these states is forbidden. The atom-field coupling constant is denoted by g (which depends only on the properties of the atomic energy levels and is independent of the light properties), N is the number of atoms in the ensemble, Ω is the Rabi frequency of the control beam (where $|\Omega|^2$ is proportional to the intensity of the control beam), and ω is the frequency detuning between the resonance of the signal and control beam (at resonance, $\omega = 0$) [6, 7, 16]. Figure 3 shows the graphs of the real and imaginary components of the susceptibility resulting from Equation 2.

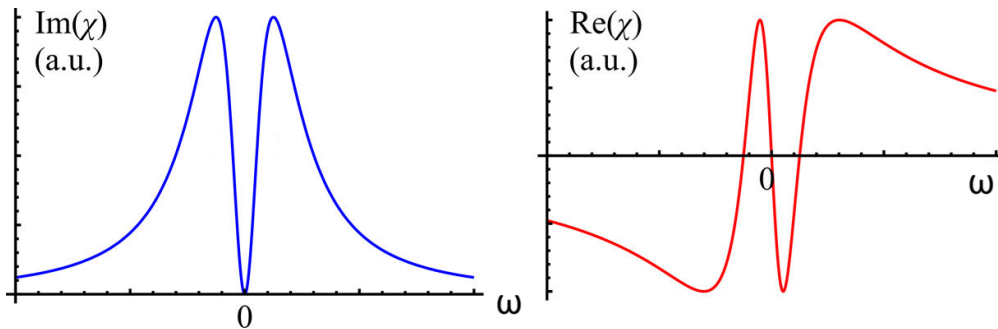


Figure 3. Linear susceptibility spectrum (in arbitrary units) of the EIT medium ($\gamma_{gs} \rightarrow 0$) for a signal beam. The real part of the susceptibility characterizes the refractive properties, the imaginary part the absorption. Adapted from [6].

We note that $\omega = 0$ corresponds to the zero value of the imaginary part of $\chi(\omega)$, which means that a narrow window of transparency appears, in which the light is not absorbed. In the same interval, the refractive index n' (see Equation 1) has a very steep gradient. Let us now recall the equations for the phase velocity of the wave (the propagation velocity of the wave fronts) and for the group velocity of the wave (the propagation velocity of the wave packets) [17]

$$v_p = \frac{\omega}{k} = \frac{c}{n'}, \quad (3)$$

$$v_g = \frac{\partial \omega}{\partial k} = \frac{c}{n' + \omega \frac{\partial n'}{\partial \omega}} \quad (4)$$

where c is the speed of light in a vacuum, n is the refractive index and ω is the frequency of light. If the refractive index does not change with the frequency, the two velocities are the same. If the refractive index changes as a function of the frequency, the group velocity is lower than the phase velocity. In the case of a very steep change, the group velocity is greatly reduced. We note that in the narrow window around $\omega = 0$, the group velocity can become significantly smaller than c due to the steep frequency dependence of the refractive index in the denominator. As we have seen, $n'(\omega)$ is very steep in this range. Let us now evaluate derivative $\frac{\partial n'}{\partial \omega}$ from Equations (1) and (2) and insert it into Equation 4 together with n' evaluated from (Equation 1). This gives us

$$v_g = \frac{c}{1 + g^2 N / |\Omega|^2}, \quad (5)$$

which clearly states that the group velocity depends on the atomic density and the intensity of the control beam. An increase in the atomic density or a decrease in the intensity of the control beam leads to a decrease in the group velocity of the signal beam. This has been demonstrated theoretically and practically (also in our laboratory). The phenomenon in question is called **slow light**. In practice, the most spectacular experimental demonstration of this ultra-slow light effect was carried out in 1999 by Hau et al. [18]. They measured a signal group velocity of 17 ms^{-1} in a Bose-Einstein condensate of sodium atoms [16].

3.2 Stored light: Dark-state polariton description

Even if we significantly reduce the speed of light, we still cannot store it. Also, we still do not have an answer to the question of how an EIT medium could preserve the full quantum state of a photon instead of just fulfilling the energy picture! It turns out that an adiabatic change in the intensity of the control beam can affect the dynamics of the signal beam with minimal losses. Furthermore, the group velocity of the signal pulse is reduced to zero when we quickly turn off the control beam, effectively storing it in the EIT medium until it is retrieved by turning the control beam back on [16]. The reduction in group velocity is also evident from Equation (5): if we set $|\Omega| \rightarrow 0$, then $v_g \rightarrow 0$.

To explain this phenomenon, we use the theory of so-called *dark-state polaritons* [19, 20]. The *dark-state polariton* is a quasiparticle, a superposition of electromagnetic waves and atomic excitations. Its quantum state $\Psi(z, t)$ is a superposition of the photonic component $E(z, t)$ and the spin component $S(z, t)$.

The development of the optical field can be described in the slowly varying amplitude approximation by the propagation equation

$$\left(\frac{\partial}{\partial t} + c \frac{\partial}{\partial z} \right) E(z, t) = - \frac{g^2 N}{\Omega(t)} \frac{\partial}{\partial t} \frac{E(z, t)}{\Omega(t)},$$

assuming that the Rabi frequency Ω changes slowly, i.e. adiabatically, and treating the equation perturbatively in E . If Ω is constant, the term on the right-hand side simply leads to a change in the group velocity of the quantum field according to Equation (5).

By introducing a new quantum field $\Psi(z, t)$ via the canonical transformation, a simple solution to this equation is then obtained

$$\Psi(z, t) = \cos \theta E(z, t) + \sin \theta S(z, t), \quad (6)$$

where

$$\cos \theta = \frac{\Omega}{\sqrt{\Omega^2 + g^2 N}}, \quad \sin \theta = \frac{g\sqrt{N}}{\sqrt{\Omega^2 + g^2 N}}. \quad (7)$$

After the signal pulse enters the EIT medium and the control beam is switched off ($\Omega \rightarrow 0$), the photonic component is reduced to 0, so that Ψ consists only of the spin component. When the control beam is switched on again, the signal is “read out” and is found to be in the same quantum state as it was initially.

Figure 4 shows a graphical representation of this process. When the control beam is switched off (time interval 50-100), the wave function only moves along the temporal dimension. At the same time, the photonic component drops to 0, while the spin component reaches its maximum value.

Around time 100 (Fig. 4 (c)), the opposite phenomenon can be observed: the wave function moves along both the temporal and spatial dimensions again, while the spin component drops to zero and the electromagnetic component reaches its maximum value. It can be seen graphically that Fig. 4 (b) is the sum of Fig. 4 (c) and Fig. 4 (d), as described in Equation (6).

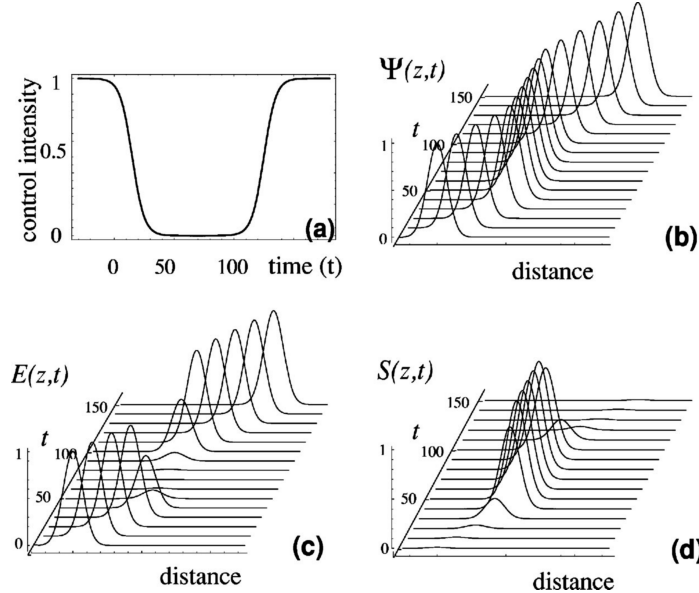


Figure 4. Graphical representation of the process of storing light. The photonic and spin parts of the dark state polariton as it passes through the EIT medium under the influence of the control beam. In the individual panels: a) temporal dependence of the control beam intensity, b) temporal and spatial dependence of the total Ψ , c) temporal and spatial dependence of the electromagnetic component, and d) temporal and spatial dependence of the spin component. Adapted form [20].

4. Quantum memory with hot Cs atoms at Laboratory for cold atoms, JSI

4.1 Hyperfine structure of cesium atom

Cesium is an alkali metal, which means that it has only one valence electron. Its only stable isotope is ^{133}Cs . The angular momentum of an atom is the sum of the electron spin \mathbf{S} , the electron orbital angular momentum \mathbf{L} , and the nuclear angular momentum \mathbf{I} . The energy levels of an atom are primarily determined by the quantum number associated with the electron orbital angular momentum \mathbf{L} . These levels are further split into the fine structure due to spin-orbit coupling, described by the total electron angular momentum $\mathbf{J} = \mathbf{L} + \mathbf{S}$. An additional splitting, known as the hyperfine structure, arises from the coupling of \mathbf{J} with the nuclear angular momentum \mathbf{I} , resulting in the total atomic angular momentum $\mathbf{F} = \mathbf{J} + \mathbf{I}$. [21, 22]

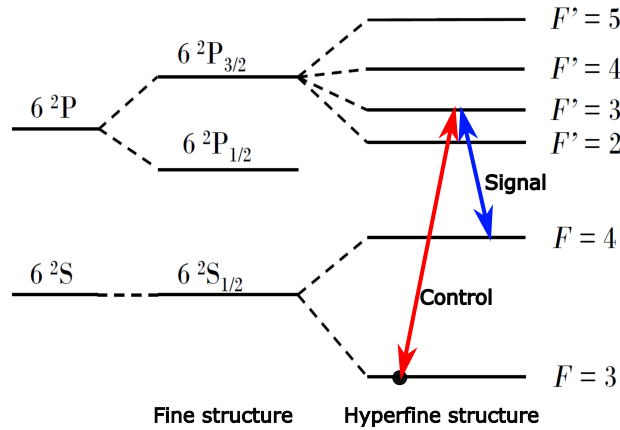


Figure 5. Energy levels of the ground state and the first excited state of ^{133}Cs atoms with control and signal transitions marked. The energy splittings are not to scale, but Λ -system discussed theoretically in Chapter 3. is clearly visible. Adapted from [21].

In the ground state of cesium, the valence electron occupies an orbital with $L = 0$ and has a spin $S = \frac{1}{2}$, which leads to a total electron angular momentum of $J = \frac{1}{2}$. Since the nuclear angular momentum of cesium is $I = \frac{7}{2}$, the hyperfine structure splits the ground state into levels with $F = 4$ and $F = 3$, with the latter having a lower energy. The energy level structure of the ground state and the first excited state of a cesium atom is illustrated in Figure 5. For our QM's Λ -system, we choose the following ^{133}Cs hyperfine structure levels: $|g\rangle = |6S_{1/2}, F = 3\rangle$, $|s\rangle = |6S_{1/2}, F = 4\rangle$, and $|e\rangle = |6P_{3/2}, F' = 3\rangle$. Precise data on these levels, chosen for control and signal transitions, is obtained from [23].

4.2 Optical setup

First, we must prepare the signal and control beams to precisely match wavelengths corresponding to $|g\rangle \rightarrow |e\rangle$ and $|s\rangle \rightarrow |e\rangle$ level transitions, respectively. We prepare them with suitable double-pass optical systems using acousto-optic modulators (AOMs) [24]. These beams are then coupled into optical fibers and transported to another optical table where the hot QM experiment is performed. Our optical setup is shown schematically in Figure 6. We obtain linearly polarized signal and control beams from optical fibers. Using $\lambda/2$ wave plates, we polarize the first beam horizontally and the second vertically. The control beam is then expanded using two lenses. Both beams are brought together at a polarizing beam splitter (PBS) and then circularly polarized with a $\lambda/4$ wave plate - one σ^+ , the other σ^- . The beams are then sent through a cesium cell located in a triple μ -metal shields, which isolate the system from the Earth's magnetic field. Inside the μ -metal shields, there are 3 orthogonal Helmholtz coils mounted centrally on the Cs cell. They can precisely generate the desired magnetic field when we perform lifetime measurements in the magnetic field. At the exit of the chamber, the beams are linearly polarized, and the control beam is filtered out with a Glan-Thompson polarizer (a type of polarizing beam splitter) so that only the retrieved signal beam is measured with a photodiode at the end of the optical line.

The time sequence of the beams with which we illuminate Cs atoms is shown in Figure 7. It is important to note that we are not working with single photons, but with classical light pulses. The AOMs that control the beams, are controlled by software written in `python`. After detection, the read signal is numerically integrated in `MATLAB`. The result is then assigned as stored light to the given storage time that we measured. We have fully automated this process, allowing us to change various parameters and repeat measurements relatively easily. We measure the influence of the magnetic field, the partial pressure of the buffer gas, and other potentially interesting parameters

on the performance of our QM.

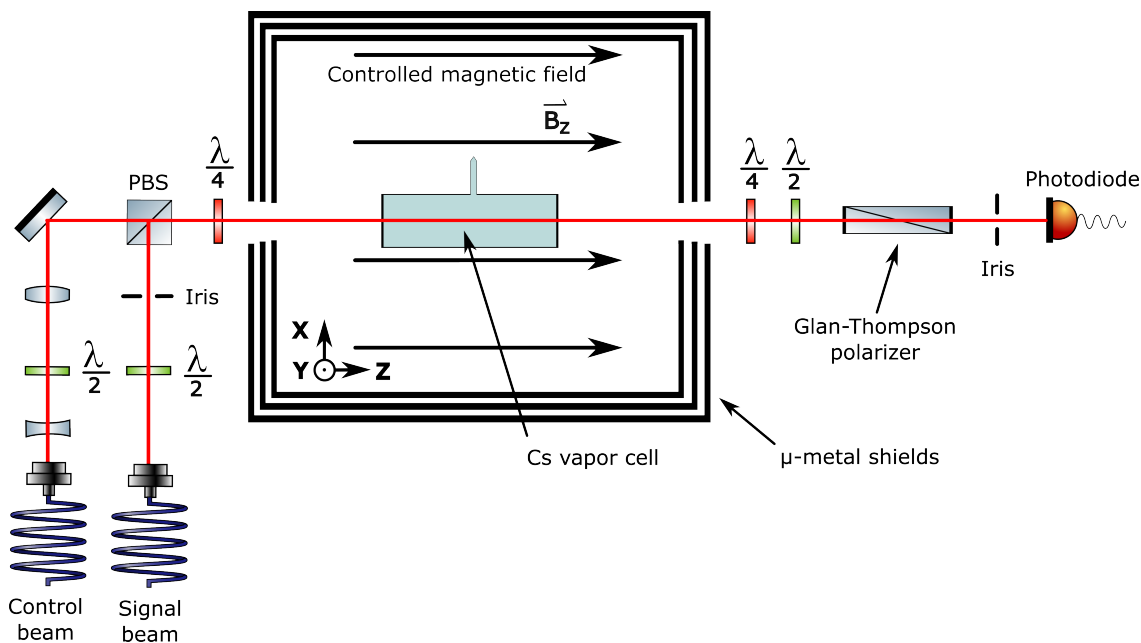


Figure 6. Setup of hot Cs atoms quantum memory experiment at Laboratory for cold atoms.

Figure 8 shows a series of measurements in which the lifetime of our QM was measured under different magnetic fields. Interesting periodic features can be observed in the results. The frequency of such periodic *revivals* and *collapses* of the stored light is proportional to the magnetic flux density.

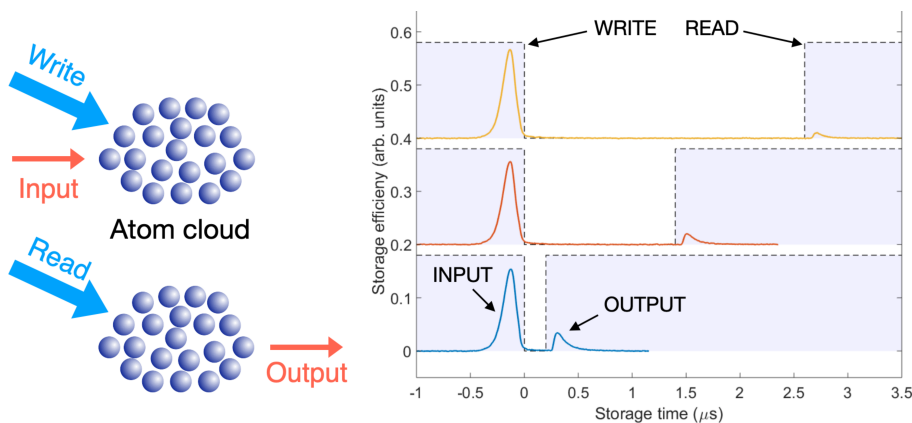


Figure 7. Graphics on the left schematically depicts our acting on the atomic ensemble, while the graphs on the right show three examples of stored light measurement sequences at three different storage times. The grey dashed line depicts the control beam sequence, where OFF time of the control beam corresponds to the storage time. The colored curves represent the signal measured by the photodiode; the first peak is leakage of the signal beam during the writing process, and the second peak (or more precisely its integral) corresponds to the stored light. The degredation of the stored light with increase of storage time can be observed from the graphs. Courtesy of Dr. Jeglič.

5. State of the art

The field of hot atoms QM is developing at a rapid pace due to increasing technological interest. Some of the best achievements in this field are a room temperature quantum memory using warm rubidium vapor, which achieves a high-fidelity retrieval (95%) at a storage time of **160 μs for single-photon operations** and up to **1 ms for classical-level light** by suppressing atomic diffusion [25].

Another significant achievement was a record **1 second** storage time QM for Cs vapor at room temperature, achieved by exploiting a decoherence-free subspace, overcoming the limitations imposed by spin-exchange collisions and outperforming previous techniques by two orders of magnitude [26]. These developments set new benchmarks for storage times and scalability, paving the way for more robust and deployable quantum memories.

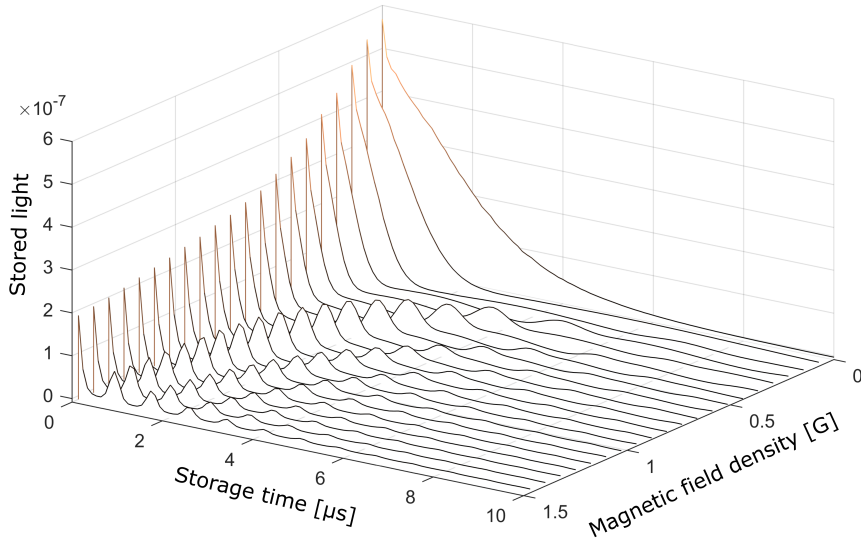


Figure 8. When doing lifetime measurement of our QM under different magnetic fields, interesting periodic features can be observed. The frequency of such periodic *revivals* and *collapses* of the stored light is proportional to the magnetic flux density [14].

6. Conclusion

This article is intended to inform the reader on the reasons why quantum memory is becoming an increasingly researched topic. An overview of the quantum memory requirements and characteristics, as well as the overview of different developing and emerging protocols for the QM has been provided. We focused on electromagnetically induced transparency and explained its theoretical background from three different perspectives that complement each other. It was explained why it is difficult to successfully store light for arbitrary periods of time and how this is done practically, including a concrete explanation of the research work being done in this field by the Laboratory for cold atoms at the Jožef Stefan Institute. Their achievements in the field of quantum memory include the successful demonstration of slowing down and storing light both in cold Cs atoms in magneto-optical trap (MOT) (storage times of more than 400 μs [14]) and hot Cs atoms (best currently achieved storage times of 5 μs). State of the art research instills hope that these results can be significantly improved in the future, which is also the main objective of our future efforts.

Acknowledgements

Since the topic of this article is motivated by and inseparably connected to the research work conducted at the Laboratory for cold atoms within the Department of Condensed Matter Physics (F5) of the Jožef Stefan Institute in Ljubljana, I cannot conclude without acknowledging all the people involved. First of all, I would like to acknowledge my colleague and coworker **Bor Luka Urlep**, who contributes equally to this experiment. Then, I would like to thank PhD students **Katja Gosar** and **Jure Pirman**, who work on their projects in the same laboratory and often provide insightful advice or help with difficulties we encounter. Last but not least, I would like to express

my sincere gratitude to **Peter Jeglič**, Head of the Laboratory for cold atoms, who makes all this research possible and is always gracefully available to direct us with his extensive expertise.

References

- [1] A. Ramšak, *Kvantna mehanika*, Fizika : zbirka fizikalnih učbenikov in monografij, Založba Univerze, Ljubljana, 2021.
- [2] *Qubit*, *Wikipedia, The Free Encyclopedia*, <https://en.wikipedia.org/wiki/Qubit> (accessed 22-December-2024).
- [3] R. Singh and R. M. Bodile, *A quick guide to quantum communication*, arXiv, ePrint, 2024.
- [4] *Quantum network*, *Wikipedia, The Free Encyclopedia*, https://en.wikipedia.org/wiki/Quantum_network (accessed 22-December-2024).
- [5] N. Sangouard, C. Simon, H. de Riedmatten, and N. Gisin, *Quantum repeaters based on atomic ensembles and linear optics*, *Rev. Mod. Phys.* **83** (2011), 33–80.
- [6] A. Nicolas, *Optical quantum memories with cold atomic ensembles : a free space implementation for multimode storage, or a nanofiber-based one for high collection efficiency*, Ph.D. thesis, Université Pierre et Marie Curie, 2014.
- [7] O. Slattery L. Ma and X. Tang, *Optical quantum memory based on electromagnetically induced transparency*, *Journal of Optics* **19** (2017), no. 4, 043001.
- [8] *Fidelity of quantum states*, *Wikipedia, The Free Encyclopedia*, https://en.wikipedia.org/wiki/Fidelity_of_quantum_states (accessed 11-December-2024).
- [9] T. B. Pittman and J. D. Franson, *Cyclical quantum memory for photonic qubits*, *Phys. Rev. A* **66** (2002), 062302.
- [10] H. P. Specht, C. Nölleke, A. Reiserer, M. Uphoff, E. Figueroa, S. Ritter, and G. Rempe, *A single-atom quantum memory*, *Nature* **473** (2011), no. 7346, 190–193.
- [11] C. Kurz, M. Schug, P. Eich, J. Huwer, P. Müller, and J. Eschner, *Experimental protocol for high-fidelity heralded photon-to-atom quantum state transfer*, *Nature Communications* **5** (2014), no. 1, 5527.
- [12] *Nitrogen-vacancy center*, *Wikipedia, The Free Encyclopedia*, https://en.wikipedia.org/wiki/Nitrogen-vacancy_center (accessed 2-January-2025).
- [13] *Quantum dot*, *Wikipedia, The Free Encyclopedia*, https://en.wikipedia.org/wiki/Quantum_dot (accessed 21-December-2024).
- [14] K. Gosar, V. Pirc Jevšenak, T. Mežnaršič, S. Beguš, T. Krehlik, D. Ponikvar, E. Zupanič, and P. Jeglič, *Suppression of dark-state polariton collapses in a cold-atom quantum memory*, *Phys. Rev. A* **108** (2023), no. 3, 032618.
- [15] *Quantum decoherence*, *Wikipedia, The Free Encyclopedia*, https://en.wikipedia.org/wiki/Quantum_decoherence (accessed 12-December-2024).
- [16] S. Mattiazzi, *Kvantni spomin za fotone*, Seminar, 2021.
- [17] I.D. Olenik and M. Vilfan, *Optika*, Fizika : zbirka fizikalnih učbenikov in monografij, vol. 6, Fakulteta za matematiko in fiziko, Ljubljana, 2023.
- [18] L. Hau, S. Harris, Z. Dutton, and C. Behroozi, *Light speed reduction to 17 metres per second in an ultracold atomic gas*, *Nature* **397** (1999), 594–598.
- [19] M. Fleischhauer and M. D. Lukin, *Dark-state polaritons in electromagnetically induced transparency*, *Phys. Rev. Lett.* **84** (2000), no. 22, 5094–5097.
- [20] M. D. Lukin, *Colloquium: Trapping and manipulating photon states in atomic ensembles*, *Rev. Mod. Phys.* **75** (2003), 457–472.
- [21] K. Gosar, *Single-shot Stern-Gerlach magnetic gradiometer with ultracold cesium atoms*, *Matrika* **7** (2020), no. 2.

- [22] T. Arh, *Nedestruktivno slikanje in magnetometrija s Faradayevo rotacijo v plinu cezijeveh atomov*, Master's thesis, Faculty of Mathematics and Physics, University of Ljubljana, 2019.
- [23] D. A. Steck, *Cesium d line data*, revision 2.3.3, 28 May 2024.
- [24] M. Čopič, M. Vilfan, and A. Petelin, *Fotonika*, Fizika : zbirka fizikalnih učbenikov in monografij, Fakulteta za matematiko in fiziko, Ljubljana, 2020.
- [25] Y. Wang, A. N. Craddock, R. Sekelsky, M. Flament, and M. Namazi, *Field-deployable quantum memory for quantum networking*, Phys. Rev. Appl. **18** (2022), 044058.
- [26] O. Katz and O. Firstenberg, *Light storage for one second in room-temperature alkali vapor*, Nature Communications **9** (2018), no. 1, 2074.